AGU PUBLICATIONS

JGR

Journal of Geophysical Research: Space Physics

RESEARCH ARTICLE
10.1002/2016JA022915

**Key Points:**
- Very oblique lower band chorus waves in magnetosphere are more commonly generated by cyclotron resonance with anisotropic electron streams
- Oblique chorus waves with large frequency chirping rates or small magnetic field amplitudes are likely excited via cyclotron resonance
- Oblique chorus waves with small frequency chirping rates or large magnetic field amplitudes are likely excited through Landau resonance

**Correspondence to:**
X. Gao,
gaoxl@mail.ustc.edu.cn

**Citation:**
Gao, X., D. Mourenas, W. Li, A. V. Artemyev, Q. Lu, X. Tao, and S. Wang (2016), Observational evidence of generation mechanisms for very oblique lower band chorus using THEMIS waveform data, *J. Geophys. Res. Space Physics*, *121*, 6732–6748, doi:10.1002/2016JA022915.

Received 5 MAY 2016
Accepted 12 JUL 2016
Accepted article online 15 JUL 2016
Published online 29 JUL 2016



# Observational evidence of generation mechanisms for very oblique lower band chorus using THEMIS waveform data

**Xinliang Gao[1,2,3], Didier Mourenas[4], Wen Li[5], Anton V. Artemyev[6], Quanming Lu[1,3], Xin Tao[1], and Shui Wang[1]**

[1]CAS Key Laboratory of Geospace Environment, Department of Geophysics and Planetary Science, University of Science and Technology of China, Hefei, China, [2]State Key Laboratory of Space Weather, Chinese Academy of Sciences, Beijing, China, [3]Collaborative Innovation Center of Astronautical Science and Technology, Harbin, China, [4]LPC2E, CNRS, University of Orleans, Orléans, France, [5]Department of Atmospheric and Oceanic Sciences, University of California, Los Angeles, California, USA, [6]Institute of Geophysics and Planetary Physics, University of California, Los Angeles, California, USA

**Abstract** Chorus waves are intense coherent whistler mode waves with frequency chirping which play a dual role in both loss and acceleration of radiation belt electrons in the Earth's magnetosphere. Although the generation of parallel chorus waves has been extensively studied by means of theory, simulations, and observations, the generation mechanism of very oblique chorus waves still remains a mystery. In this study, we have analyzed hundreds of very oblique discrete (rising or falling tone) lower band chorus events collected from 7 years of Time History of Events and Macroscale Interactions during Substorms (THEMIS) waveform data to investigate their potential generation mechanisms. Comparisons between wave normal angles directly measured onboard THEMIS in the dawn-day sector at $L = 5$–$9$ and inferred from theoretical models on the basis of measured wave characteristics (frequency sweep rate, mean frequency, and amplitude) show that these very oblique waves are more commonly generated through cyclotron resonance with anisotropic electron streams. However, a second generation mechanism via Landau resonance with low-energy electron beams seems to be also operating on the nightside at $L < 6.7$ and at all local times at $L > 8.5$. Moreover, very oblique lower band chorus waves with large frequency chirping rates or small magnetic field amplitudes are more likely excited via cyclotron resonance, while waves with small frequency chirping rates or large magnetic field amplitudes are preferentially generated through Landau resonance. This comprehensive statistical study provides interesting insight into the possible generation mechanisms of very oblique lower band chorus waves in the Earth's magnetosphere.

## 1. Introduction

Whistler mode chorus waves have long been a topic of active research in the community of magnetospheric physics, due to their important role in the overall dynamics of the Earth's radiation belt and their unique properties. Chorus waves are considered as the dominant driver of diffuse auroral precipitation through pitch angle scattering of low-energy (0.1–30 keV) electrons [*Thorne et al*., 2010; *Ni et al*., 2011]. Furthermore, chorus waves are generally believed to be important to produce relativistic radiation belt electrons through rapid local acceleration [*Summers et al*., 2002; *Thorne et al*., 2013]. One of the most remarkable properties of chorus waves is their frequency chirping, appearing as either rising tones or falling tones in high time resolution dynamic spectrograms [e.g., *Li et al*., 2012; *Gao et al*., 2014a, and references therein]. Another distinct feature is the remarkable power gap at about 0.5 $f_{ce}$ ($f_{ce}$ is the electron gyrofrequency) [*Tsurutani and Smith*, 1974], which separates the chorus emission into two bands: a lower band ($<0.5\ f_{ce}$) and an upper band ($>0.5\ f_{ce}$).

Chorus waves are typically detected in the vicinity of the magnetic equator ($|\mathrm{MLAT}| < 10°$, where MLAT is the magnetic latitude) [*LeDocq et al*., 1998; *Santolik et al*., 2005; *Li et al*., 2009], which has been recognized as their main source region. It has been widely accepted that chorus waves are excited through linear and nonlinear resonant interactions with hot and anisotropic electrons (tens of keV) injected from the plasma sheet during substorms [*Nunn*, 1971; *Karpman et al*., 1974; *Omura et al*., 2008, 2012; *Shklyar and Matsumoto*, 2009; *Li et al*., 2010; *Demekhov*, 2011; *Omura and Nunn*, 2011; *Nunn and Omura*, 2012; *Gao et al*., 2014b; *Nunn and Omura*, 2015]. By considering the relativistic second-order resonant condition, *Omura et al*. [2008] found that the evolution of wave frequencies and amplitudes of chorus waves is controlled by the nonlinear resonant current

resulting from resonant electron trapping into the effective potential generated by the wave electric field and the mirror force acting together on particles in the inhomogeneous geomagnetic field [see *Trakhtengerts et al.*, 2004]. They further successfully reproduced parallel propagating lower band rising tones with a 1-D PIC (Particle In Cell) simulation model. Moreover, this theory also indicates that chorus waves should be excited under some optimum condition [*Hikishima and Omura*, 2012], which was supported by the THEMIS observations [*Gao et al.*, 2014b]. For upper band chorus waves, many potential mechanisms have been proposed to explain their generation and also the power gap at about 0.5 $f_{ce}$, such as a strong damping at about 0.5 $f_{ce}$ [*Omura et al.*, 2009], different free energy sources [*Fu et al.*, 2014], and the lower band cascade [*Gao et al.*, 2016].

Although chorus waves are usually observed with small wave normal angles ($<45°$) near the magnetic equator [*Li et al.*, 2011a, 2013], very oblique chorus waves have also been reported in many previous works [*Agapitov et al.*, 2013; *Li et al.*, 2013, 2016; *Mourenas et al.*, 2014; *Artemyev et al.*, 2015], especially for falling tones [*Li et al.*, 2011b, 2012]. Moreover, both theoretical and observational results have shown that very oblique chorus waves are able to induce more efficient losses of energetic electrons ranging from ~30 keV to ~ 1 MeV than quasi-parallel chorus waves due to strong higher-order cyclotron resonances [*Mourenas et al.*, 2012; *Li et al.*, 2014; *Artemyev et al.*, 2015, 2016]. Ray tracing simulations have indicated that a population of oblique chorus waves could be formed during wave propagation from the geomagnetic equator toward the higher-latitude region due to magnetic gradients and curvature [*Chen et al.*, 2013]. Moreover, very oblique lower band chorus waves have high occurrences even near the geomagnetic equator [*Santolik et al.*, 2009; *Li et al.*, 2013, 2016; *Agapitov et al.*, 2013; *Mourenas et al.*, 2014; *Taubenschuss et al.*, 2014], indicating that they should be excited there with very large wave normal angles. However, the exact generation mechanism of such very oblique lower band chorus waves still remains a mystery.

Recently, *Mourenas et al.* [2015] and *Artemyev et al.* [2016] have analytically examined two possible generation mechanisms for very oblique chorus waves based on the second-order resonance condition: Landau resonance with low-energy electron beams and cyclotron resonance with anisotropic electron streams. *Mourenas et al.* [2015] and *Artemyev et al.* [2016] derived three simplified approximate formulae (respectively, equations (19) and (20) and equation (72) in these papers) corresponding to wave generation via Landau or cyclotron resonances under different assumptions, each formula providing a distinctive theoretical relationship between the wave frequency chirping rate and the wave normal angle. However, a comprehensive statistical analysis of very oblique chorus events is required to evaluate the validity of such simplified nonlinear models of very oblique wave generation in the Earth's magnetosphere. By analyzing nearly 7 year THEMIS (Time History of Events and Macroscale Interactions during Substorms) waveform data, we have been able to investigate the potential generation mechanisms of intense very oblique lower band chorus waves on the basis of these models, studying in particular how wave properties relate to their possible generation mechanism. In section 2, we describe the analysis of THEMIS waveform data and the three frequency chirping rate formulae used in this study. The statistical properties of very oblique lower band chorus events and comparisons of wave-normal angles inferred from theoretical models and directly from observations are presented in section 3. In section 4, we summarize and further discuss our principal results.

## 2. THEMIS Data Analysis and Theoretical Formulae

The very oblique lower band chorus waves studied in this paper are recorded by three inner THEMIS spacecraft (A, D, and E) [*Angelopoulos*, 2008], which are ideally located to detect chorus waves in the near-equatorial magnetosphere. The chorus waves can be detected by the Search-Coil Magnetometer (SCM) [*Le Contel et al.*, 2008] and the Electric Field Instrument (EFI) [*Bonnell et al.*, 2008], which simultaneously provide multiple 6–8 s waveform data each day with a sampling frequency of up to ~ 16 kHz. Meanwhile, we can obtain polarization properties of very oblique lower band chorus in this study by analyzing the high-resolution waveform data (scw and efw files). The background magnetic fields are calculated by taking a 16 data point (4 s) sliding average on the low-resolution FGM (Fluxgate Magnetometer) data (4 Hz) [*Auster et al.*, 2008], which are then utilized to estimate the equatorial electron gyrofrequency for a roughly dipolar geomagnetic field (at locations most often far away from the possibly strongly disturbed midnight sector; see section 3). To exclude chorus events inside the plasmapause, the background plasma density inferred from the spacecraft potential and electron thermal speed [e.g., *Li et al.*, 2010] has been required to remain lower than 30 $cm^{-3}$, as in previous studies [*Li et al.*, 2010, 2013; *Gao et al.*, 2014a].

After converting the waveform data into the field-aligned coordinate system ($z$ axis is along the background magnetic field), we use three components of magnetic fluctuations to calculate the detailed polarization parameters (such as wave-normal angle $\theta$, polarization ratio $R_p$, and ellipticity) of chorus waves with a time resolution of ~0.016 s following the procedure developed by *Bortnik et al.* [2007]. For waves with sufficiently large polarization ratios ($R_p > 0.9$), the obtained polarization parameters are highly reliable [*Bortnik et al.*, 2007]. Since chorus waves in the magnetosphere are normally highly polarized and typically have right-handed polarization, the waves and polarization parameters are recorded only when $R_p > 0.9$ and ellipticity $> 0.7$. Because there is an inherent 180° ambiguity in the calculated wave-normal angle by using three components of magnetic field alone, all the wave-normal angles have been converted into values less than 90°.

Recently, *Mourenas et al.* [2015] and *Artemyev et al.* [2016] have studied two possible generation mechanisms of intense very oblique chorus waves in the Earth's magnetosphere. The first one relies on Landau resonance with low-energy (<4 keV) electron beams either injected from the plasma sheet during substorms or locally generated by some acceleration processes. The second-generation mechanism is based on cyclotron resonance with low-energy (<15 keV) streams: the free energy for wave growth can then come from a realistic temperature anisotropy $T_\perp/T_{||} \sim 1.5$–$2.5$ of antiparallel (to the waves) keVs electrons, aided by a simultaneous reduction of Landau damping from lower energy (100 s eV) electrons (propagating in the same direction as the waves) provided by a local plateau, or heavy tail, in the parallel velocity distribution (such distributions may be symmetric). Due to significant uncertainties of wave-normal angle measurements at large $\theta$, generally within the magnitude of 3°–5° [*Taubenschuss et al.*, 2014; *Mourenas et al.*, 2015], it is often difficult to assess whether $\theta$ remains roughly constant or varies over the duration of one wave event. Thus, one may assume either a nearly constant $\theta$ or else a monotonously varying $\theta$ during nonlinear wave growth. Under the first assumption of a nearly constant $\theta$ (corresponding for instance to the maximum linear and nonlinear growth rates) during the nonlinear generation process taking place near the magnetic equator, and for $\theta$ sufficiently close to the resonance cone (for $f_{ce}\cos\theta/f - 1 < 0.3$ and $\theta > 60°$), *Mourenas et al.* [2015] derived two simplified formulae (their equations (19) and (20)) for the frequency chirping rates corresponding to Landau or cyclotron resonance, which can be readily employed for analyzing satellite observations. These two formulae are rewritten below (see Appendix A for details):

$$\frac{\partial\omega}{\partial t} \approx \pm 2^{3/2} S^* \omega^2 \left(\frac{B_{w0}}{B_0}\right) \frac{(\cos\theta - \cos\theta_r)}{\cos\theta_r} \tag{1}$$

$$\frac{\partial\omega}{\partial t} \approx \pm 2^{3/2} S^* \omega^2 \left(\frac{B_{w0}}{B_0}\right) \frac{(\cos\theta - \cos\theta_r)\omega^2}{\cos\theta_r (\Omega_{ce} - \omega)^2} \tag{2}$$

where equations (1) and (2) are for Landau and cyclotron resonances, respectively. Here $\omega$, $B_{w0}$, $\Omega_{ce}$, and $B_0$ are the mean wave frequency, mean wave amplitude, electron gyrofrequency, and background magnetic field intensity, respectively. The resonance cone angle $\theta_r$ is defined by $\cos\theta_r \approx \omega/\Omega_{ce}$ in the cold plasma approximation. The term $S^*$ (~0.6) is the optimum inhomogeneity ratio [e.g., see *Omura et al.*, 2008; *Shklyar and Matsumoto*, 2009] maximizing nonlinear wave growth at the equator (see Appendix A and *Mourenas et al.* [2015]). Under the alternative assumption of a monotonously varying $\theta$ during the nonlinear process of very oblique wave growth, *Artemyev et al.* [2016] derived similar formulae. They found that a Landau resonance generation mechanism led to unrealistically large frequency chirping rates, while generation via cyclotron resonance yielded realistic levels. The latter case corresponds to another useful formula, given below for $\Omega_{ce}\cos\theta/\omega - 1 < 0.3$ and $\theta > 60°$ (see Appendix A for more details):

$$\frac{\partial\omega}{\partial t} \approx \pm S^* \left(\frac{B_{w0}}{B_0}\right) \frac{\omega^6}{\sqrt{2}(\cos\theta - \cos\theta_r)\Omega_{ce}^4 \cos\theta} \tag{3}$$

In this study, the above three approximate formulae are used to investigate potential generation mechanisms of very oblique lower band chorus waves, by comparing wave-normal angles directly measured by THEMIS with those inferred from the three very different formulae on the basis of the measured frequency chirping rate, mean wave frequency, wave amplitude, and geomagnetic field amplitude. Although the above formulae are only approximate (within factors ~1.5–2 of exact values), their simplified form is indeed convenient to infer $\theta$ from the measured frequency chirping rate and wave amplitude. Hereafter, these three formulae, i.e., equations 1–3, are called as *L*, C1, and C2 for convenience. In future works, it would be interesting to use

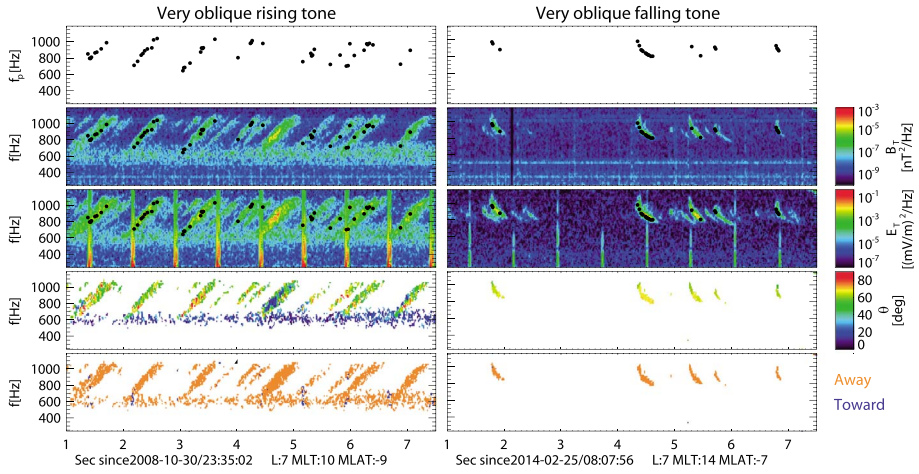


**Figure 1.** (first row) Peak frequency $f_p$ with the maximum magnetic spectral density. (second and third rows) Magnetic and electric frequency-time spectrograms. (fourth row) The wave-normal angle $\theta$ for very oblique (left column) rising and (right column) falling tones, respectively. (fifth row) The wave-propagating direction (orange means away from the equator, while blue denotes toward the equator). The frequency range of the vertical axis is from 0.1 to 0.5 $f_{ce}$.

the full equations of motion [e.g., *Nunn and Omura*, 2015] to compare each observation with corresponding numerical simulations to get more precise insights.

## 3. Observational Results

In the present study, the waveform data obtained from 1 June 2008 to 1 June 2015 by the three inner probes (THEMIS A, D, and E) are analyzed to collect very oblique lower band chorus events over the radial distance from 5 to 9 $R_E$ at magnetic latitudes less than 10° (within the typical source region). Two representative examples of very oblique lower band chorus waves are displayed in Figure 1 to explain how to select the chorus event. From top to bottom, Figure 1 shows the peak frequency $f_p$ with the maximum magnetic spectral density at each time, magnetic and electric frequency-time spectrograms, wave normal angle $\theta$, and wave propagating direction for very oblique rising (left column) and falling (right column) tones. With the same method by *Li et al.* [2013], the wave propagating direction is inferred from both directions of Poynting flux and the radial component of the background magnetic field. Here orange color denotes propagating away from the magnetic equator, while blue color means propagating toward the magnetic equator. At each time, the peak frequency $f_p$ is kept only when the data point meets the following criteria. First, the wave magnetic field amplitude $B_T$ must be larger than 8 pT (thereby excluding reflected chorus waves, whose amplitudes are generally smaller than 5 pT; see *Parrot et al.* [2003], *Agapitov, et al.* [2011], *Kurita et al.* [2012], *Li et al.* [2013], and *Breuillard et al.* [2014]). Here $B_T$ is obtained by integrating the magnetic spectral density over the frequency from $f_p - 32$ Hz to $f_p + 32$ Hz due to the narrow bandwidth of discrete chorus waves [*Gao et al.*, 2014a]. Second, the wave normal angle $\theta$ must be sufficiently large ($>60°$) and very close to the resonance cone angle (i.e., $\Omega_{ce}\cos\theta/\omega - 1 < 0.3$). Moreover, only a discrete (rising or falling tone) lower band chorus element containing at least three adequate data points is recorded as one very oblique lower band chorus event. For example, we could obtain only seven rising tones and three falling tones in Figure 1. Meanwhile, the wave normal angle $\theta$, wave frequency $f$, wave normal angle changing rate $d\theta/dt$, wave frequency chirping rate $df/dt$, mean wave amplitude $B_T$, and background magnetic field intensity $B_0$ are also recorded for each chorus event.

The resulting global distribution of very oblique rising tones (left; red) and falling tones (right; blue) is illustrated in Figure 2. In our database, there are about 200 rising tones and 300 falling tones. As shown in Figure 2 (left), very oblique rising tones preferentially occur from predawn to afternoon sector, while very oblique falling tones are usually detected from midnight to noon sector (Figure 2, right). Moreover, for both very oblique rising and falling tones, events on the nightside are generally located at smaller L shells ($<$7–7.5) than on the dayside. We caution, however, that the relatively less frequent observations on the nightside over 22–04 MLT stem in part from the MLT distribution of waveform measurements on THEMIS, which were available more often on the dayside at $< 9\ R_E$. Figure 3 shows an overview of comparisons between wave normal

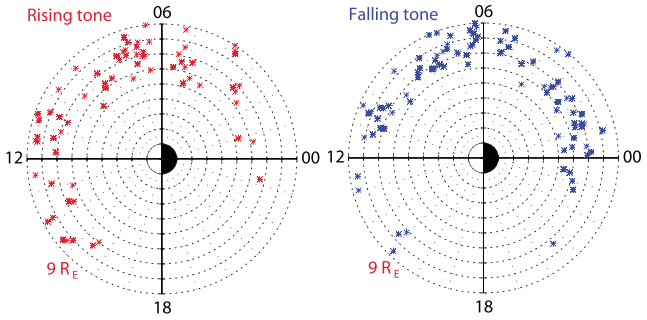


**Figure 2.** The global distribution of very oblique lower band (left; red) rising tones and (right; blue) falling tones. Each star denotes one chorus event.

angles directly measured on THEMIS and inferred from theoretical models on the basis of measured wave frequency chirping rate and amplitude, for both rising (red) and falling (blue) tones. Each star represents one chorus event. The $\theta_L$, $\theta_{C1}$, and $\theta_{C2}$ in Figure 3 are calculated from *L*, C1, and C2 by inputting all the other measured parameters (wave magnetic field amplitude, frequency chirping rate, mean wave frequency, and geomagnetic field strength) for each event. The observed wave normal angle $\theta_o$ for each event is the weighted average of $\theta$ by wave magnetic field amplitudes. Under the assumption of nearly constant $\theta$ in Figures 3a, 3b, 3d, and 3e, for both rising and falling tones, the formula *L* provides much better agreement with measured values than the formula C1, suggesting that Landau resonance with low-energy beams may be a potential generation mechanism of very oblique lower band chorus waves. Note that there are significantly less events shown in Figures 3b and 3e, because formula C1 leads to unrealistic results for a number of events. However, as shown in Figures 3c and 3f, under the alternative assumption of a monotonously varying $\theta$, the formula C2 provides even better predictions of wave normal angle values for the majority of very oblique chorus events. This result is quite fascinating, because it indicates that cyclotron resonance with anisotropic electron streams may be the more common generation mechanism for very oblique lower band chorus waves.

It is interesting to investigate whether the assumption of a nearly constant $\theta$ is actually valid for very oblique chorus events in the magnetosphere. Therefore, the discrepancies ($\delta\theta_L$, $\delta\theta_{C1}$, and $\delta\theta_{C2}$) between wave normal angles inferred from the simplified theoretical models and directly measured are exhibited in Figure 4 as a function of the wave normal angle changing rate $\mathrm{d}\theta/\mathrm{d}t$ for both rising (red) and falling (blue) tones. The dashed lines represent the median values, with the first and third quartiles shown by vertical bars. Taking formula *L* as an example, $\delta\theta_L$ is defined as $\sqrt{\sum_{i=1}^{N}\left(\theta_L^i-\theta^i\right)^2/N}$ (where *N* is the number of data points for each event) to quantitatively evaluate theoretical results. As shown in Figures 4a, 4b, 4d, and 4e, both $\delta\theta_L$ and $\delta\theta_{C1}$ increase with the increase of $\mathrm{d}\theta/\mathrm{d}t$ for both rising and falling tones. This is exactly consistent with the expected behavior, since both the *L* and C1 formulae rely on an assumption of nearly constant $\theta$ which becomes invalid when $\mathrm{d}\theta/\mathrm{d}t$ is sufficiently large (typically for $\mathrm{d}\theta/\mathrm{d}t > 15°/\mathrm{s}$, corresponding to $\Delta\theta > 5°$ over a wave event). Comparing with Figures 4c and 4f, it appears that $\delta\theta_{C2}$ becomes sensibly larger than $\delta\theta_L$ for $\mathrm{d}\theta/\mathrm{d}t < 15°/\mathrm{s}$ for several rising and falling tone events, implying that such events are more likely produced through Landau resonance rather than via cyclotron resonance. Conversely, for $\mathrm{d}\theta/\mathrm{d}t > 15°/\mathrm{s}$, wave generation through cyclotron resonance (C2 formula) becomes clearly prevalent.

We have further examined how the properties of the waves relate to their potential generation mechanisms. Figure 5 illustrates the discrepancies ($\delta\theta_L$, $\delta\theta_{C1}$, and $\delta\theta_{C2}$) between wave normal angles directly measured and inferred from theoretical models, as a function of the frequency chirping rate $\mathrm{d}f/\mathrm{d}t$ for both rising (red) and falling tones (blue). The dashed lines represent the median values, with the first and third quartiles shown in vertical bars. The most striking result is that the discrepancy $\delta\theta_L$ is very small (less than 3°–5°, i.e., less than the typical measurement uncertainty ~5°) when the frequency chirping rate is smaller than ~300 Hz/s, especially for very oblique falling tones (Figure 6d). Moreover, there is a clear trend of increasing $\delta\theta_L$ and $\delta\theta_{C1}$ as the frequency chirping rate increases, for both rising (Figures 5a and 5b) and falling tones (Figures 5d and 5e). Conversely, the discrepancy $\delta\theta_{C2}$ gradually decreases for falling tones as their frequency chirping rate $\mathrm{d}f/\mathrm{d}t$ increases from about 50 Hz/s to 0.5–1 kHz/s in Figures 5c–5f, generally remaining at a level sensibly larger than $\delta\theta_L$ over the whole range $\mathrm{d}f/\mathrm{d}t < 0.5$–1 kHz/s, while becoming much smaller for $\mathrm{d}f/\mathrm{d}t > 1$ kHz/s. The median value of $\delta\theta_{C2}$ is also larger than the median value of $\delta\theta_L$ in the domain $\mathrm{d}f/\mathrm{d}t < 0.3$ kHz/s for rising tones, while it becomes smaller for $\mathrm{d}f/\mathrm{d}t > 1$ kHz/s. Consequently, we find that very oblique lower band chorus events with large frequency chirping rates can better be explained by a generation mechanism via

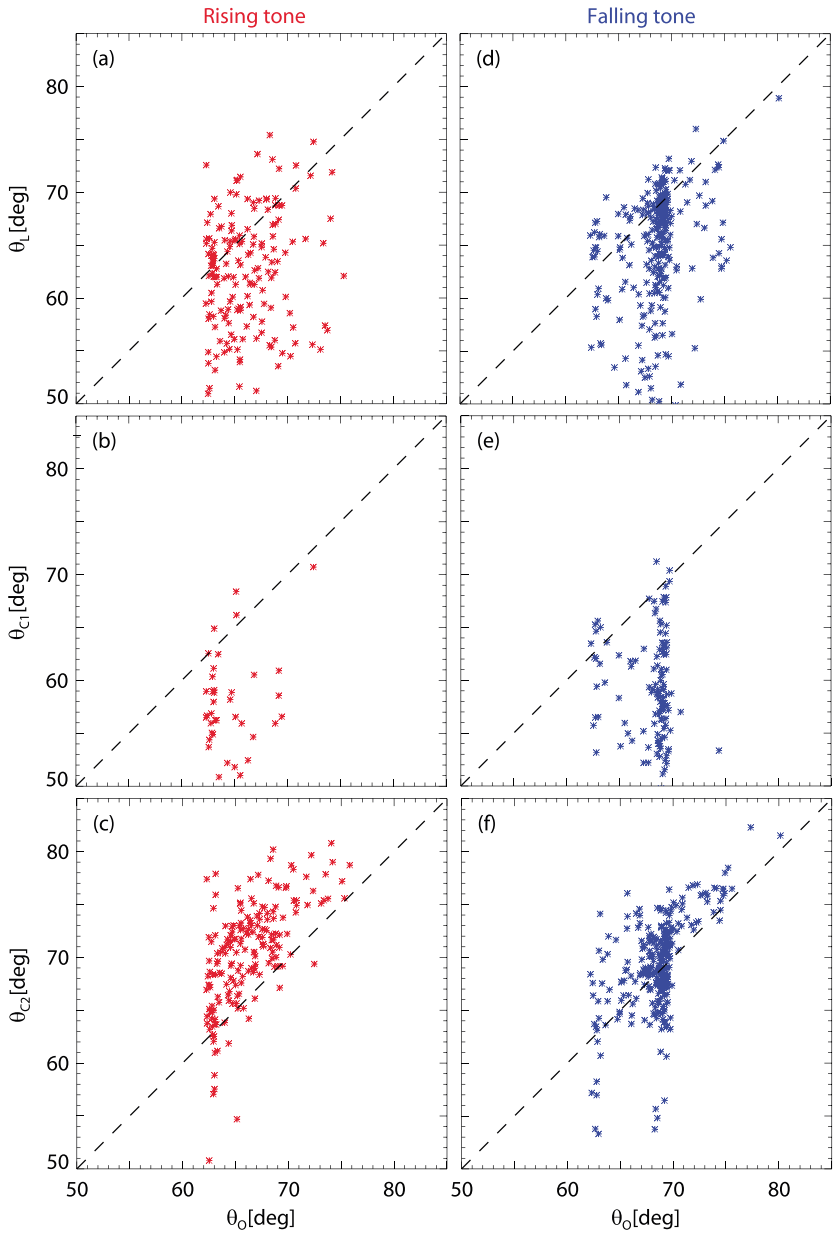


**Figure 3.** Comparisons between wave-normal angles inferred from simplified theoretical models ((a, d) $\theta_L$, (b, e) $\theta_{C1}$, and (c, f) $\theta_{C2}$) and directly measured ($\theta_o$) for both rising (red) and falling (blue) tones. Each star represents one chorus event. The $\theta_L$, $\theta_{C1}$, and $\theta_{C2}$ are obtained from formulae *L*, C1, and C2, respectively.

cyclotron resonance with anisotropic electron streams. On the other hand, very oblique chorus waves with small frequency chirping rates are preferentially generated through Landau resonance with low-energy electron beams.

The dependence on the wave amplitude $B_T$ of the discrepancies ($\delta\theta_L$, $\delta\theta_{C1}$, and $\delta\theta_{C2}$) between wave normal angles directly measured and inferred from simplified theoretical models is also evaluated, and displayed in Figure 6 for both rising (red) and falling (blue) tones. Under the assumption of a nearly constant wave-normal angle, both $\delta\theta_L$ and $\delta\theta_{C1}$ decrease as the mean wave amplitude increases from 8 pT up to 30–60 pT, for both rising and falling tones in Figures 6a, 6b, 6d, and 6e. There is also a slight increasing trend of $\delta\theta_{C2}$ as the wave amplitude increases above 40 pT for falling tones in Figure 6f. For both rising (Figures 6a and 6c) and falling tones (Figures 6d and 6f), when the wave amplitude becomes sufficiently large ($>$50 pT), the discrepancy $\delta\theta_L$ remains at a very low level, while $\delta\theta_{C2}$ becomes larger than $\delta\theta_L$ for falling tones, indicating that more intense

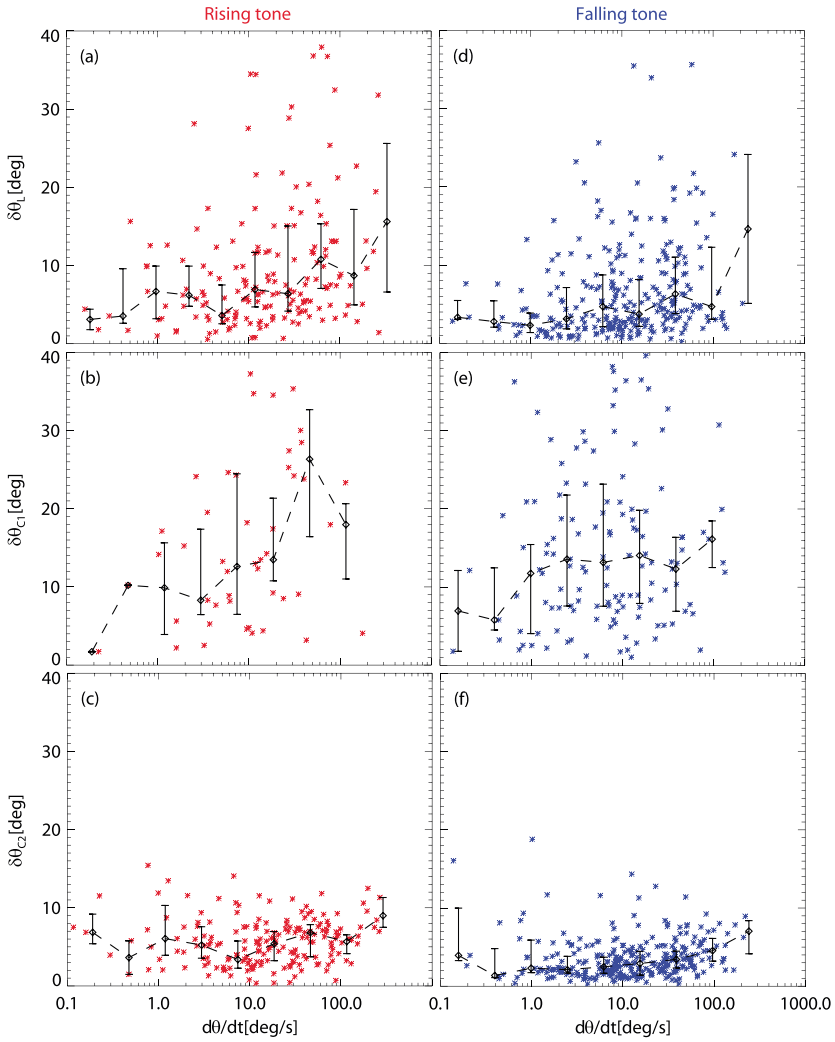


**Figure 4.** The discrepancies ((a, d) $\delta\theta_L$, (b, e) $\delta\theta_{C1}$, and (c, f) $\delta\theta_{C2}$) between wave-normal angles directly measured by THEMIS and inferred from simplified theoretical models, as a function of the wave-normal angle changing rate d$\theta$/d$t$ for both rising (red) and falling (blue) tones, respectively. Here each star represents one chorus event. In each panel, the dashed line represents the median values, with the first and third quartiles shown in vertical bars.

falling tones are preferentially excited through Landau resonance. Conversely, very oblique waves with small amplitudes (<30 pT) are clearly more likely generated through cyclotron resonance.

To investigate whether the very oblique chorus events that can be explained by Landau resonance (*L*) or cyclotron resonance (C2) represent two distinct types of events, the distribution of rising (red) and falling (blue) tones has been plotted in the $\delta\theta_L$ - $\delta\theta_{C2}$ domain in Figure 7. Except for a small (very small) portion of rising (falling) tones with simultaneously large $\delta\theta_L$ (>6°–7°) and $\delta\theta_{C2}$ (>6°–7°), almost all very oblique lower band chorus events can be explained by either Landau resonance (*L*) or cyclotron resonance (C2) generation. Note that more chorus events have a small $\delta\theta_{C2} < 7°$ than a small $\delta\theta_L < 7°$, suggesting that a generation mechanism via cyclotron resonance may be more common, which is consistent with the results shown in Figure 3. A small but noticeable portion of falling and rising tones, with simultaneously small $\delta\theta_L < 7°$ and large $\delta\theta_{C2} > 7°$, can only be generated via Landau resonance. However, there is a larger portion of falling and rising tones, with simultaneously large $\delta\theta_L > 7°$ and small $\delta\theta_{C2} < 7°$, which can only be generated via cyclotron resonance. It is also worth noting the neat separation between two falling tone populations of events for $\delta\theta_L$ and $\delta\theta_{C2} > 5°$: such events are located far from the diagonal in Figure 7b and constitute two well-separated populations such that either $\delta\theta_L < 7°$ or $\delta\theta_{C2} < 7°$. This is a clear manifestation of the existence of two distinct generation mechanisms (via either Landau or cyclotron resonance) corresponding to two distinct populations of very oblique wave events.

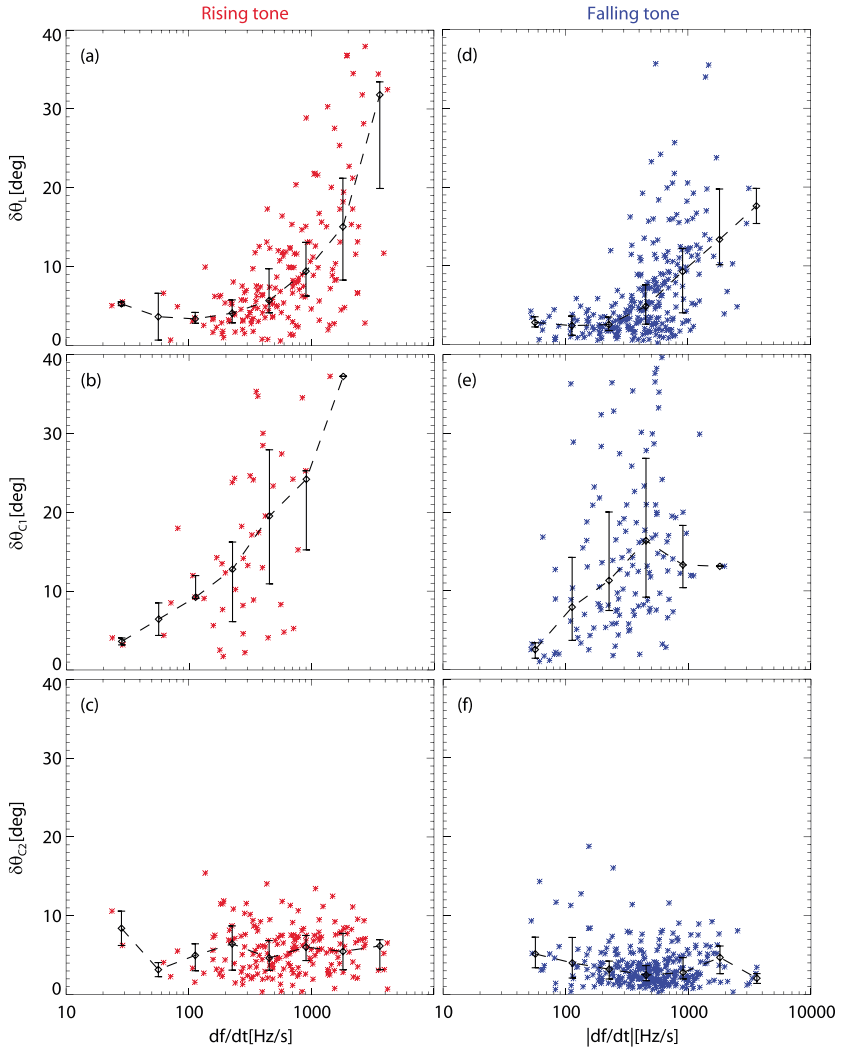


**Figure 5.** The differences ((a, d) $\delta\theta_L$, (b, e) $\delta\theta_{C1}$, and (c, f) $\delta\theta_{C2}$) between wave-normal angles directly measured by THEMIS and inferred from simplified theoretical models, as a function of the frequency changing rate d*f*/d*t* for both rising (red) and falling (blue) tones, respectively. Here each star represents one chorus event. In each panel, the dashed line represents the median values, with the first and third quartiles shown by vertical bars.

Accordingly, falling (or rising) tone very oblique chorus wave events have been divided into two groups: more Landau-like events $F_L$ (or $R_L$) with $\delta\theta_L < \delta\theta_{C2}$ and more cyclotron-like events $F_C$ (or $R_C$) with $\delta\theta_L > \delta\theta_{C2}$. The different properties of these two groups are studied in Figure 8, which displays the distributions in both L-MLT (Figures 8a and 8c) and $\theta_o$-$B_T$ (Figures 8b and 8d) domains for the two groups. Triangles denote the more Landau-like events, while plus signs denote the more cyclotron-like events. Although the majority of chorus events in these two groups overlap in Figure 8, there are still two things worth noting. At $L = 5$–6.7 (i.e., inside the outer radiation belt), 60% of cyclotron-like events take place over 23–05 MLT and 40% over 05–14 MLT, while 75% of more Landau-like events occur over 23–05 MLT. Although the total number of such events at $L = 5$–6.7 is small (~60), it suggests that generation via Landau resonance occurs preferentially on the nightside in this region, while generation through cyclotron resonance occurs more uniformly in MLT. At $L > 8.5$, Landau-like events turn out to represent 60% of the total number of events at all MLT (from 0 to 15 MLT), showing that very oblique chorus waves are more likely generated via Landau resonance with low-energy electron beams than through cyclotron resonance with anisotropic populations in this region of the magnetosphere. Figures 8b and 8d further show that very oblique waves with large magnetic field amplitudes are more likely to be generated via Landau resonance, especially for falling tones.

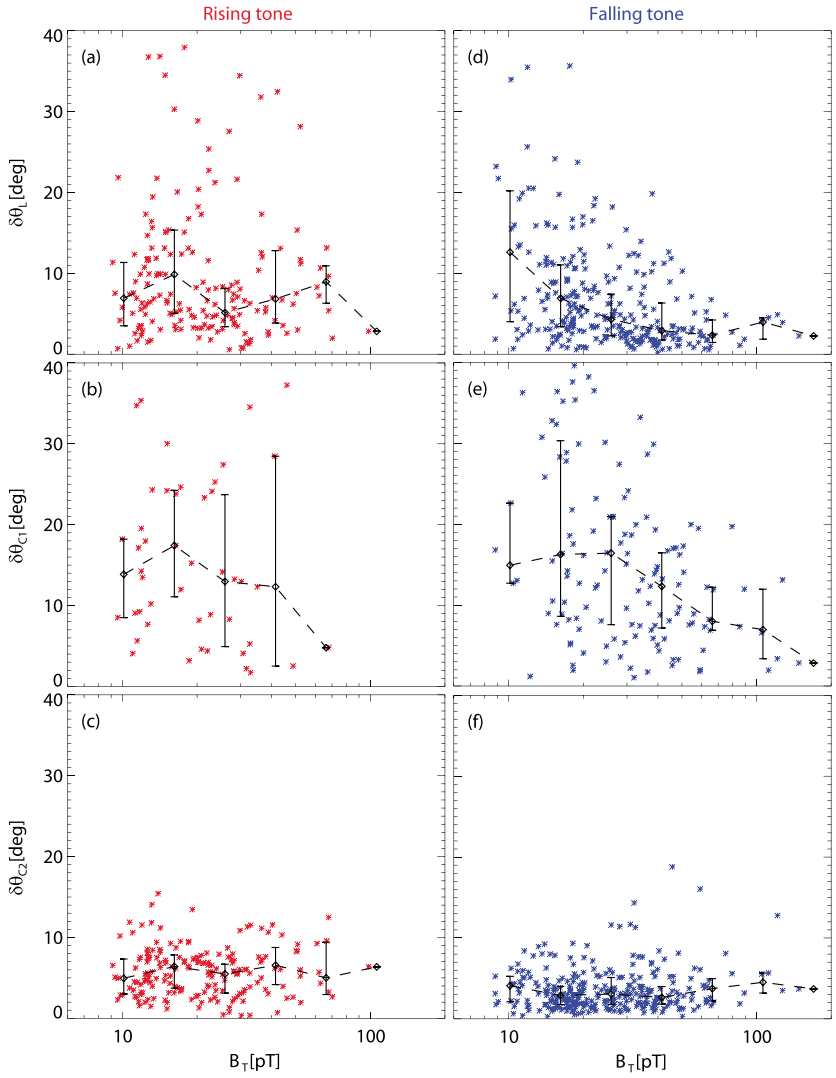


**Figure 6.** The differences ((a, d) $\delta\theta_L$, (b, e) $\delta\theta_{C1}$, and (c, f) $\delta\theta_{C2}$) between wave-normal angles directly measured by THEMIS and inferred from simplified theoretical models, as a function of the wave magnetic amplitude $B_T$ for both rising (red) and falling (blue) tones, respectively. Here each star represents one chorus event. In each panel, the dashed line represents the median values, with the first and third quartiles shown in vertical bars.

## 4. Summary and Discussion

We have analyzed hundreds of very oblique discrete (rising or falling tone) lower band chorus events near the geomagnetic equator collected from the multiyear waveform data of the three inner THEMIS probes to investigate their potential generation mechanisms based on recent theoretical studies by *Mourenas et al*. [2015] and *Artemyev et al*. [2016]. This comprehensive statistical study may provide interesting insight into the potential generation mechanisms of very oblique lower band chorus waves in the Earth's magnetosphere. We can summarize the principal results as follows:

1. During many very oblique lower band chorus events, the wave normal angle varied significantly together with the wave frequency. It suggests that a mechanism of wave generation via cyclotron resonance with anisotropic electron streams is generally more likely at $L = 5–9$ in the dawn-day sector as a whole.
2. Comparisons between wave normal angles directly measured by THEMIS and inferred from simple theoretical models of nonlinear generation (on the basis of measured wave frequency chirping rates and amplitudes) show that nearly all very oblique lower band chorus events can be explained by these simplified models, either via Landau resonance with low-energy electron beams or through cyclotron

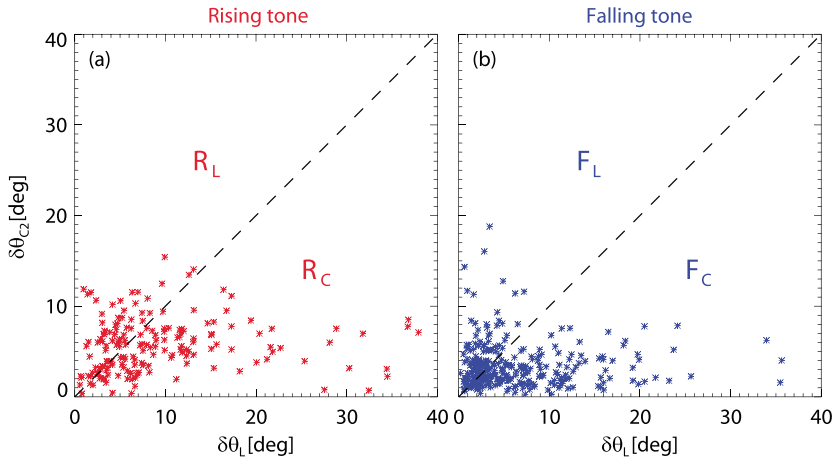


**Figure 7.** The distribution of (a) rising (red) and (b) falling (blue) tones in the $\delta\theta_L$ - $\delta\theta_{C2}$ domain. Each star represents one chorus event. The events have been divided into two groups by the dashed lines: more Landau-like events $R_L$ (or $F_L$) with $\delta\theta_L < \delta\theta_{C2}$ and more cyclotron-like events $R_C$ (or $F_C$) with $\delta\theta_L > \delta\theta_{C2}$.

resonance with anisotropic electron streams. However, very oblique lower band chorus waves may be slightly more commonly generated via cyclotron resonance with anisotropic electron populations in the considered region of the Earth's magnetosphere.

3. A significant portion of falling tone events (as well as a smaller portion of rising tones) can be clearly split into two distinct groups, each group corresponding to a preferential generation mechanism (via either cyclotron or Landau resonance).
4. Very oblique lower band chorus waves with small frequency chirping rates or large magnetic field amplitudes are preferentially generated through Landau resonance with low-energy electron beams, especially in the 23–05 MLT sector at $L = 5$–$6.7$ and at all local times at $L > 8$–$8.5$.
5. Very oblique lower band chorus waves with large frequency chirping rates or small magnetic field amplitudes are more likely excited by cyclotron resonance with anisotropic electron streams in the region $L < 8$.

In this study, we have considered two possible generation mechanisms for very oblique chorus waves, via Landau or cyclotron resonances, which were proposed by *Mourenas et al.* [2015] and *Artemyev et al.* [2016]. To further confirm the viability of the two above possible generation regimes, we have used linear theory [*Kennel and Engelman*, 1966] to numerically calculate growth rates of very oblique whistler mode waves. Such linear growth rate calculations assume a homogeneous geomagnetic field, and they are only valid during the early, initial stage of wave growth from noise level in the close vicinity of the equator (over the first ~0.1 s). As soon as waves reach amplitudes sufficient for trapping to occur, nonlinear effects must be properly taken into account in wave growth, as well as magnetic field inhomogeneity (e.g., see Appendix A). Figure 9 (left column) exhibits the product of the normalized growth rate $\Gamma/\Omega_{ce}$ multiplied by the relative density of resonant electrons $\overline{n}$ as a function of the wave normal angle $\theta$, while Figure 9 (right column) displays the corresponding parallel (solid line) and transverse (dashed line) electron distributions. Note that the parallel (transverse) electron distributions represent the electron phase space density (PSD) values near 0° (90°) pitch angle. Here $n = 0$, $n = -1$, and $\Sigma$ denote Landau resonance, cyclotron resonance, and their sum, respectively. The considered resonant electron distribution function $f_{res} = f_{st} + f_{hot} + f_{beam}$ is a combination of three distribution functions (suprathermals, hot, and beam, respectively) with

$$f_{st} = n_{st}\frac{1}{\pi^{3/2}v_{Tst}^3}\exp\left(-\frac{v^2}{v_{Tst}^2}\right)$$

$$f_{hot} = n_{hot}\frac{C_k}{\pi^{3/2}k^{3/2}v_{Th||}^2 v_{Th\perp}}\left(1+\frac{v_{||}^2}{kv_{Th||}^2}+\frac{v_{\perp}^2}{kv_{Th\perp}^2}\right)^{-k-1}$$

$$f_{beam} = n_{beam}\frac{1}{2\pi^{3/2}v_{Tb}^3}\exp\left(-\frac{v_{\perp}^2}{v_{Tb}^2}\right)\left(\exp\left(-\frac{(v_{||}-v_{beam})^2}{v_{Tb}^2}\right)+\exp\left(-\frac{(v_{||}+v_{beam})^2}{v_{Tb}^2}\right)\right)$$

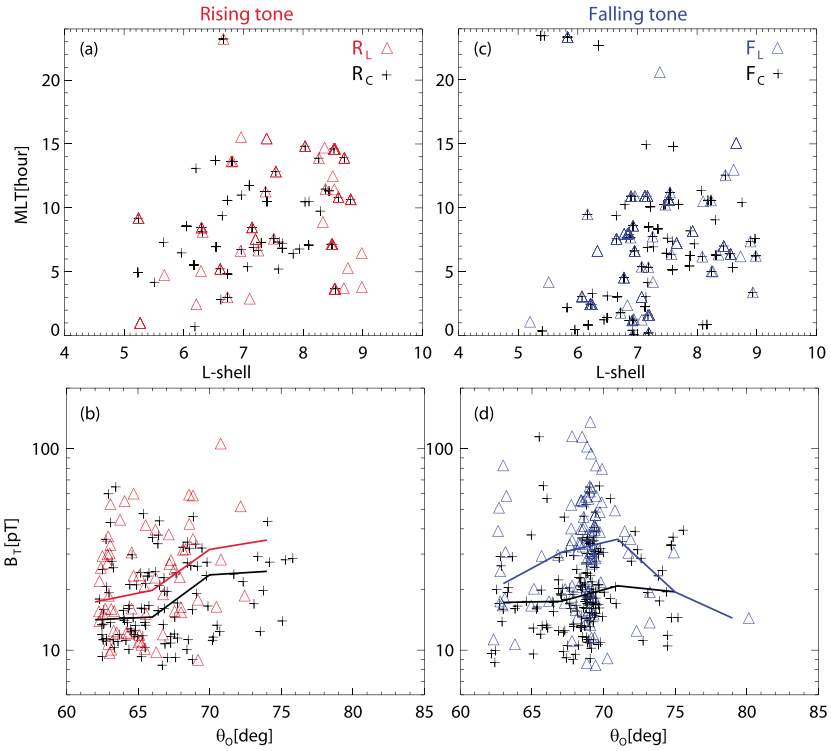


**Figure 8.** Distributions of very oblique (left column) rising and (right column) falling tones in both (a, c) MLT-L shell and (b, d) $B_T$–$\theta_o$ domains for both the more Landau-like and cyclotron-like events. Triangles denote more Landau-like events, while plus signs denote the more cyclotron-like events. Horizontal lines in Figures 8b and 8d denote the median wave amplitude $B_T$ for Landau-like (red or blue line) and cyclotron-like (black lines) events.

and $C_k$ is a normalization constant. We chose very typical parameters in the Earth's radiation belt, which are $k=3$, $n_{st}/n_{hot}=10$, $T_{st}=m_e v_{Tst}^2/2=200$ eV, $T_{beam}=m_e v_{Tb}^2/2=500$ eV, $T_{hot,||}=m_e v_{Th||}^2/2=4$ keV, $v_{beam}/v_{Tb}=2$, and wave frequency $\omega=0.35\Omega_{ce}$. The ratio of the plasma frequency to electron gyrofrequency is set as $\Omega_{pe}/\Omega_{ce}=4.5$. Three cases (from top to bottom) have been considered: (1) $n_{beam}/n_{hot}=1$, $v_{Th\perp}^2/v_{Th||}^2=1.4$; (2) $n_{beam}/n_{hot}=0.25$, $v_{Th\perp}^2/v_{Th||}^2=2.0$; and (3) $n_{beam}/n_{hot}=0.1$, $v_{Th\perp}^2/v_{Th||}^2=2.4$.

In the first case (Figure 9, top row), the electron beam is strong enough to produce a positive slope in the parallel velocity distribution function, which leads to $\Gamma_{n=0}>0$ at the large wave normal angle $\theta\sim65°$ through Landau resonance. However, the anisotropy of hot electrons is too weak to produce a positive growth rate by cyclotron resonance. In the second case (Figure 9, middle row), the positive slope in the parallel distribution function is slightly reduced, but the temperature anisotropy of hot electrons is enhanced. As a result, both Landau and cyclotron resonances may lead to the generation of oblique whistler mode waves. In the third case (Figure 9, bottom row), there is only a plateau in the parallel velocity distribution function, due to the weak electron beam, which suppresses the Landau damping at large wave normal angles. In this case, the generation of oblique whistler mode waves is only provided by the cyclotron resonance ($\Gamma_{n=-1}>0$ at $\theta$ ~60°–65°) with the hot anisotropic population. As shown in Figure 7, there are many very oblique lower band chorus events having both small $\delta\theta_L$ and small $\delta\theta_{C2}$, which implies that both Landau and cyclotron resonances could be operating during the corresponding generation processes. Based on the above calculations shown in Figure 9 (middle row), we can speculate that the energetic electrons injected from the plasma sheet during substorms are more likely to have a velocity distribution similar to this second case. Meanwhile, events with large $\delta\theta_{C2}$ and small $\delta\theta_L$ may be excited via Landau resonance with a strong low-energy electron beam as in the first case of Figure 9. Events with large $\delta\theta_L$ and small $\delta\theta_{C2}$ could be generated through cyclotron resonance with anisotropic hot electrons, as in the third case.

A determination of the global distribution of low-energy electron beams in the Earth's magnetosphere would be helpful to better understand our statistical results of more Landau-like events in Figure 8, but there are still no clear statistical results due to the limitations of low-resolution plasma measurements. However, we may

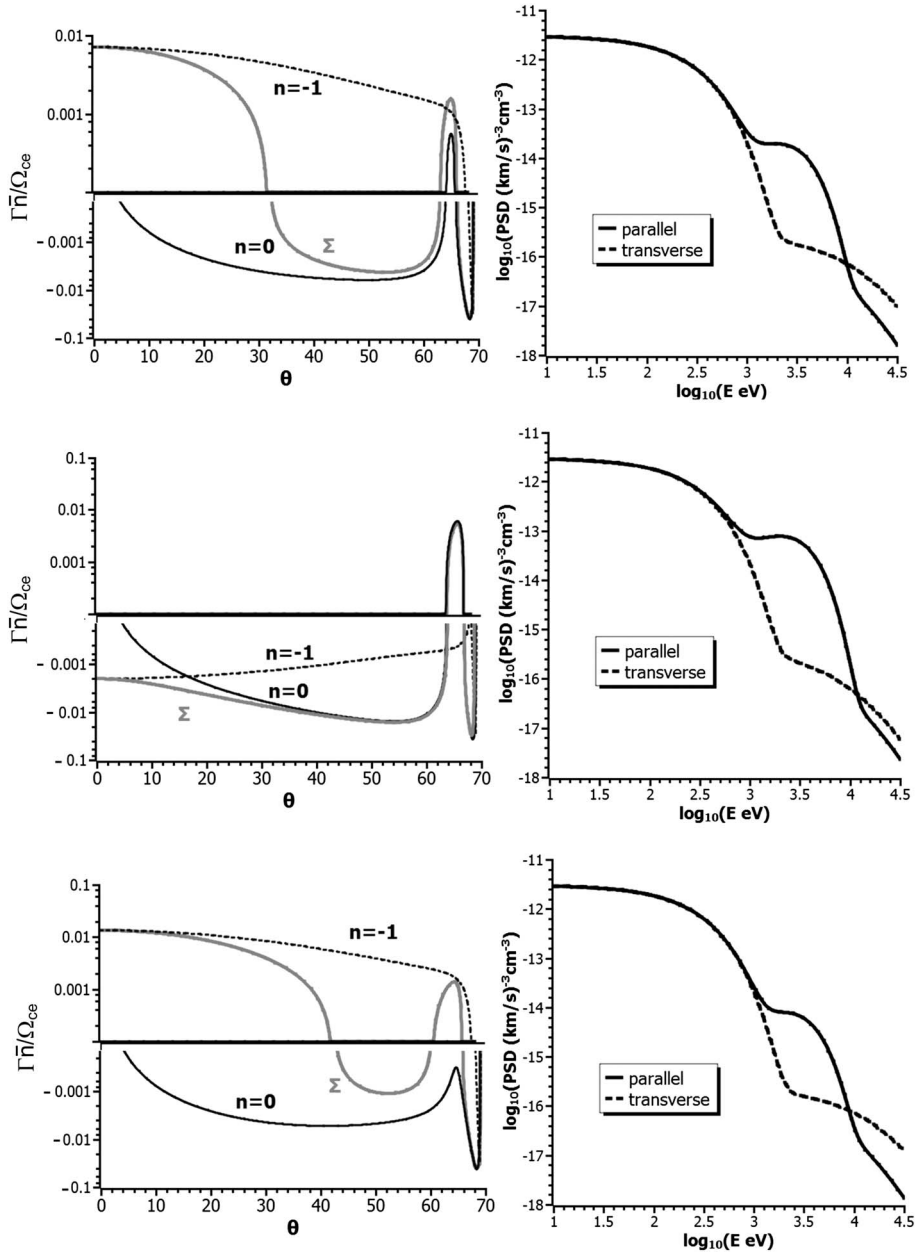


**Figure 9.** (left column) The product of the normalized growth rate $\Gamma/\Omega_{ce}$ multiplied by the relative density of resonant electrons $\overline{n}$ as a function of the wave-normal angle $\theta$; (right column) the parallel (solid line) and transverse (dashed line) electron PSD (phase space density; $(\mathrm{km/s})^{-3}\mathrm{cm}^{-3}$) as a function of the kinetic energy $E$ (eV) for the three cases described in the text, respectively. Here $n = 0$ (black solid lines), $n = -1$ (black dashed lines), and $\Sigma$ (gray solid lines) denote Landau resonance, cyclotron resonance, and their sum, respectively.

get a clue from a recent statistical study about TDS (time domain structures) [*Malaspina et al*., 2015], which are frequently observed along with electron beams [*Mozer et al*., 2015]. As shown in Figure 8, nearly all more Landau-like oblique chorus events within $L < 7$ occur from 20 to 10 MLT, which corresponds to the region where TDS have been detected [*Malaspina et al*., 2015]. At $L > 8$, electron beams could probably exist even on the dayside due to various acceleration processes [*Williams et al*., 1985; *Hall et al*., 1991; *Kletzing*, 1994; *Lee et al*., 1994], which is also consistent with our statistical results in Figure 8. Actually, electron beams are expected to excite also Langmuir waves and to relax under their influence toward a plateau. However, very oblique whistler mode waves can still manage to grow over a short period before the beam is fully flattened [e.g., *An et al*., 2016]. In the magnetosphere, beam and plasma inhomogeneities as well as low-frequency

turbulence can reduce Langmuir wave growth and efficiently slow down beam relaxation (e.g., see discussion in *Mourenas et al*. [2015]), probably explaining their observations. Moreover, particle injections from the plasma sheet are often accompanied by strong field-aligned electron beams generated by local acceleration mechanisms [e.g., *Zheng et al*., 2012]. Examining the difference between the electron distributions related to more Landau-like and cyclotron-like chorus events would be important and helpful to understand the generation of chorus waves, but the analysis of electron distribution functions at low energies (100 eV to 5 keV) is not trivial, since it requires selecting periods when spacecraft potential does not alter measurements and where sudden injections or convection do not modify the distributions. Moreover, the resolution in THEMIS data is relatively low. Also, "averaged" patterns may not correspond to given rising or falling tones of much shorter duration (a few tenths of seconds). Therefore, it would require comprehensive and careful investigations. For these reasons, we have decided to focus in this first paper on wave data, leaving a detailed examination of particle distributions for another separate study.

## Appendix A: Derivation of Approximate Frequency Sweep Rate Formulae

We consider the propagation of very oblique, quasi-electrostatic lower band chorus whistler mode plane waves along geomagnetic field lines and their interactions with low-energy electrons of $E < 5-10$ keV via first-order cyclotron or Landau resonances, which are generally the most efficient resonances [*Shklyar and Matsumoto*, 2009; *Omura et al*., 2015]. Our goal here is merely to estimate the wave frequency sweep rate in the generation region [e.g., see *Omura et al*., 2008; *Omura and Nunn*, 2011]. For this limited task, we can restrict our consideration to the close vicinity of the magnetic equator and neglect plasma density inhomogeneity. Many observational studies have indeed pointed out that intense chorus waves (including oblique waves) mostly propagate away from the geomagnetic equator [*Kurita et al*., 2012; *Li et al*., 2013; *Agapitov et al*., 2015].

To further reduce the complexity of the problem, we focus only on very oblique waves such that $\Omega_{ce}\cos\theta/\omega - 1 < 0.3$ with a wave-normal angle $\theta > 60°$ and a frequency $\omega$ much higher than the lower hybrid frequency and smaller than half of the electron gyrofrequency $\Omega_{ce}$, in a region such that $\Omega_{pe}/\Omega_{ce} > 4$ (with $\Omega_{pe}$ the electron plasma frequency). It allows using a simplified cold plasma dispersion relation

$$\frac{k^2c^2}{\omega^2} \approx \frac{\Omega_{pe}^2}{\omega(\Omega_{ce}\cos\theta - \omega)} \tag{A1}$$

with $k$ the wave number and $c$ the velocity of light.

For plane wave propagation in a uniform medium, with slowly varying phase, $\omega$, $k$, and $\theta$, conservation of the wave characteristic frequency and parallel wave number in a frame moving at the wave's group velocity $V_{g||} = \partial\omega/\partial k_{||}$ along the $z$ axis parallel to the magnetic field line corresponds to relations

$$\begin{aligned} \frac{\partial\omega}{\partial t} + V_{g||}\frac{\partial\omega}{\partial z} &= 0 \\ \frac{\partial k_{||}}{\partial t} + V_{g||}\frac{\partial k_{||}}{\partial z} &= 0 \end{aligned} \tag{A2}$$

Based on satellite observations in the generation region generally showing small variations of $\theta$ remaining within the uncertainty range (≈5°) of measurements [*Taubenschuss et al*., 2014; *Mourenas et al*., 2015], two different hypotheses can be made concerning the behavior of $\theta$ during the nonlinear wave generation process: it may either be taken as roughly constant (for instance, at a value corresponding to maximum linear and nonlinear growth) or be allowed to vary smoothly. In the first case, one may approximate $V_{g||} \sim V_g k/k_{||}$, leading to

$$V_{g||} \approx \frac{2c\Omega_{ce}}{\Omega_{pe}}\frac{(\Omega_{ce}\cos\theta - \omega)^{3/2}\omega^{1/2}}{\Omega_{ce}^2}c^{ce}os^2\theta \tag{A3}$$

In the second case, the full expression of $V_{g||}$ can be simplified for $\Omega_{ce}\cos\theta/\omega - 1 < 0.3$ and $\theta > 60°$, leading to

$$V_{g||} \approx \frac{c\Omega_{ce}}{\Omega_{pe}}\frac{(\Omega_{ce}\cos\theta - \omega)^{1/2}\omega^{3/2}}{\Omega_{ce}^2}c^{ce}os^2\theta \tag{A4}$$

The velocity of electrons in Landau (or Cerenkov) resonance with the wave is equal to the parallel phase velocity $\omega/k_{||}$ of the wave and given by

$$V_{R||,0} \approx \frac{c\sqrt{\omega(\Omega_{ce}\cos\theta - \omega)}}{\Omega_{pe}\cos\theta} \tag{A5}$$

In the case of first-order cyclotron resonance, the larger but negative resonant velocity $V_{R||,1}$ can be written as

$$V_{R||,1} \approx \frac{c\sqrt{\omega(\Omega_{ce}\cos\theta - \omega)}}{\Omega_{pe}\cos\theta}\frac{\omega - \Omega_{ce}}{\omega} \tag{A6}$$

Let us now consider the evolution of the parallel velocity $v_{||}$ of low-energy electrons interacting resonantly with these waves. For a given Landau ($n = 0$) or first-order cyclotron ($n = 1$) resonance, the relevant equation of motion is given by equation (37) from *Nunn and Omura* [2015]:

$$\frac{dv_{||}}{dt} \approx \frac{\omega_{t,n}^2 \sin\eta_n}{k_{||}} - \frac{v^2 \sin^2\alpha}{2\Omega_{ce}}\frac{\partial\Omega_{ce}}{\partial z} \tag{A7}$$

with $m_e$ the electron mass, $\alpha$ its pitch angle, and $\eta_n$ the generalized phase between the wave and the particle. The corresponding trapping frequencies $\omega_{t,n}$ can be written as a function of wave field components as

$$\begin{aligned} \frac{m_e\omega_{t,0}^2}{ek_{||}} &= E_w\cos\theta J_0(\beta) - v_\perp B_{w,x} J_1(\beta) \\ \frac{m_e\omega_{t,1}^2}{ek_{||}} &= E_w\cos\theta J_1(\beta) + v_\perp J_0(\beta)\frac{B_{w,x} + B_{w,y}}{2} \end{aligned} \tag{A8}$$

where $\beta = k_\perp v_\perp/\Omega_{ce}$.

Combining dispersion relation with Landau resonance condition, one gets $\beta \approx \tan\theta\tan\alpha\omega/\Omega_{ce}$. Moreover, strong wave growth via Landau resonance requires abundant electrons. For a given resonant parallel velocity, it corresponds mainly to $\alpha < 45°$. For the considered very oblique waves, it leads to $\beta < 0.8$ and therefore $J_1/J_0 < 0.5$. Making use again of the Landau resonance condition and dispersion relation to replace $v_\perp = v_{||}\tan\alpha$, and using relationships between wave field components provided by *Verkhoglyadova et al.* [2010], one finds that for $\Omega_{ce}\cos\theta/\omega - 1 < 0.3$, the first right-hand side term in equation (A8) for $\omega_{t,0}$ is much larger than the second term, giving $\omega_{t,0} \approx (ek_{||}E_w\cos\theta/m_e)Z_0$ with $Z_0 \approx J_0(\beta) - J_1(\beta)\beta(\Omega_{ce}\cos\theta/\omega - 1) \approx J_0(\beta) \sim 1$. Thus, a reasonable approximation is $\omega_{t,0} \approx ek_{||}E_w\cos\theta/m_e$. The strongest wave-particle coupling via Landau resonance indeed occurs near the maximum of the corresponding Bessel function $J_0$, i.e., for $J_0(\beta < 0.7) \approx 1$.

Considering cyclotron resonance condition with dispersion relation, one gets similarly $\beta \approx \tan\theta\tan\alpha(\Omega_{ce} - \omega)/\Omega_{ce}$. The most efficient wave-particle coupling via first-order cyclotron resonance occurs near the maximum of the corresponding Bessel function $J_1$, i.e., for $J_1 \approx 0.6$ when $\beta$ lies between 1.4 and 2. Considering $\omega/\Omega_{ce} \sim 0.3 - 0.4$ (the main frequency range of very oblique lower band chorus waves; see *Li et al.* [2016]), such values of $\beta$ can be reached for $\alpha$ in the range $30° - 60°$ (i.e., the usual range for optimum wave growth via temperature anisotropy; e.g., see *Nunn and Omura* [2015]). Replacing as before the wave field and velocity components in equation (A8) for $\omega_{t,1}$, one finds $\omega_{t,1} \approx (ek_{||}E_w\cos\theta/m_e)Z_1$ with $Z_1 \sim J_1(\beta) + \beta J_0(\beta)(\Omega_{ce}\cos\theta/\omega - 1)/\sqrt{2}\cos\theta\sin^2\theta$. Considering optimum wave-particle coupling, one gets $Z_1$ about 0.7 to 1.1 for some $\beta$ between 1.4 and 2 when $\Omega_{ce}\cos\theta/\omega - 1 \sim 0.05 - 0.25$. Thus, one can reasonably use $Z_1 \sim 1$ as a first-order approximation.

Assuming that the resonance condition is satisfied, the derivative of the generalized phase $\eta_n$ between the wave and the particle is given by $d\eta_n/dt = k_{||}(v_{||} - V_{R||,n}) = 0$, leading to a second-order resonance condition

$$\frac{d^2\eta_n}{dt^2} = k_{||}\frac{d}{dt}\left(v_{||} - V_{R||,n}\right) \tag{A9}$$

Using equations (A1)–(A6), one can express $dV_{R||,n}/dt$ in equation (A9) as a function of the $\omega$ and $k_{||}$ variations seen by an electron moving at $v_{||}$: $d\omega/dt = (1 - v_{||}/V_{g||})\partial\omega/\partial t$, $dk_{||}/dt = (1 - v_{||}/V_{g||})\partial k_{||}/\partial t + \sigma_n\partial\Omega_{ce}/\partial z$, and $d\Omega_{ce}/dt = v_{||}\partial\Omega_{ce}/\partial z$. Using also equation (A7), one obtains a second-order nonlinear differential equation

describing the dynamics of electrons in Landau or cyclotron resonance with the wave [e.g., *Omura and Nunn*, 2011; *Omura et al*., 2012; *Nunn and Omura*, 2015]

$$\frac{\mathrm{d}^2\eta_n}{\mathrm{d}t^2} = \omega_{t,n}^2(\sin\eta_n + S_n) \tag{A10}$$

where the inhomogeneity factor $S_n$, defined as the ratio of inhomogeneity to oscillatory terms, can be written as

$$\omega_{t,n}^2 S_n = \left(1 - \frac{V_{R||,n}}{V_{g||}}\right)^2 \frac{\partial\omega}{\partial t} + \xi_n \frac{\partial\Omega_{ce}}{\partial t} \tag{A11}$$

and approximate expressions for $\xi_n$ have been provided in *Mourenas et al*. [2015].

For electron trapping in the wave potential and nonlinear wave growth to exist, a necessary condition is $|S_n| < 1$ [e.g., *Shklyar and Matsumoto*, 2009; *Omura et al*., 2012]. Following the approach of *Shklyar and Matsumoto* [2009], here we take into account the presence of both trapped and transient electron populations exchanging energy with the waves. Considering asymptotic behavior ($t\omega_{t,n} > 1$), *Shklyar and Matsumoto* [2009] have shown that the nonlinear growth rate $\gamma_{\mathrm{NL}}$ depends on $S_n^2$, i.e., the sign of $\gamma_{\mathrm{NL}}$ depends on the sign of the difference between energy variations of untrapped and trapped populations, or equivalently on the sign of the derivative of the unperturbed population near resonance, but not on the sign of the inhomogeneity $S_n$ (However, if the impact of transient particles can be omitted, $\gamma_{\mathrm{NL}}$ depends linearly on $S_n$; see *Omura et al*. [2008]). Thus, we hereafter use $S = S_n \equiv |S_n|$. Equation (4.26) from *Shklyar and Matsumoto* [2009] provides a general expression for $\gamma_{\mathrm{NL}}$ based on an evaluation of the resonant current for cyclotron or Landau resonance:

$$\gamma_{\mathrm{NL}} = \gamma_L \frac{16}{\pi^2} \Phi^{3/2} \left\langle \Phi^{1/2} \Gamma_T S \int S(t)\mathrm{d}t \right\rangle \tag{A12}$$

where $\gamma_L$ is the linear growth rate, $\Phi$ is a dimensionless coefficient depending on particle energy and pitch angle [see *Shklyar and Matsumoto*, 2009], $\Gamma_T$ is the phase space volume of trapped particles surrounded by the separatrix of system (A10), and the average is a weighted average over transverse adiabatic invariant with weight $\partial f_0/\partial W|_{v_{||}=V_{R||}}$, with $W$ the particle energy and $f_0$ the electron distribution function. The integral inside the weighted average is performed over the timescale $\Delta t$ of resonant interaction. Taking into account that resonance width is small in velocity space, one may approximate equation (A12) as

$$\gamma_{\mathrm{NL}} \approx \gamma_L \frac{16}{\pi^2} \Phi^2 S^2 \Gamma_T \Delta t \tag{A13}$$

where the function $\Gamma_T$ has a form [e.g., *Artemyev et al*., 2012]

$$\Gamma_T = \oint \eta \mathrm{d}\eta = 2\omega_t \sqrt{S} \int_{\eta_-}^{\eta_+} \sqrt{H_\eta + S^{-1}\cos\eta - \eta}\,\mathrm{d}\eta = 2\omega_{t,n}\sqrt{S}R(S) \tag{A14}$$

with $H_\eta = \eta_- - S^{-1}\cos\eta_-$ the energy of the nonlinear pendulum (A10); $\eta_-$ is a solution of equation $\sin\eta = -S\eta$, and $\eta_+$ is a solution of equation $H_\eta + S^{-1}\cos\eta - \eta = 0$. As shown by *Mourenas et al*. [2015], a reasonable approximation for $R(S)$ is $R(S) \approx (5/2)(S^{-1} - 1)$, leading finally to

$$\gamma_{\mathrm{NL}} \approx \gamma_L \frac{80}{\pi^2} \omega_t \Delta t \Phi^2 \left(S^{3/2} - S^{5/2}\right) \tag{A15}$$

As the nonlinear growth rate (A15) reaches its maximum around $S = S^* \approx 3/5$, we may assume that nonlinear wave growth maximizes for $S \sim S^*$. Further assuming that nonlinear wave growth takes place in the very close vicinity of the equator (where $\partial\Omega_{ce}/\partial z = 0$), the approximate formulae (1)–(3) for the frequency sweep rate given in the main text can be easily derived from equation (A11), using equation (A3) or (A4) for $V_{g||}$ appropriate for each case, with (A5) or (A6) for resonant velocities and approximated equations (A8) for $\omega_{t,0}$ or $\omega_{t,1}$, finally switching from $E_w$ to full wave magnetic amplitude $B_w$ (using equation (13) from *Verkhoglyadova et al*. [2010]) for $\theta$ near the resonance cone. No comparisons are displayed in the present paper between the observed frequency sweep rates and the sweep rate formula obtained for Landau resonance in case of a varying $\theta$ [*Artemyev et al*., 2016, equation (70)]. This is because the latter approximate formula yielded unrealistically high values in this case. Nevertheless, it does not necessarily imply that this case does not exist: waves excited with such very large $\partial\omega/\partial t$, over very short timescales, may not be easily identified in wave data.

Note that the frequency sweep rate formulae derived here are only *approximate* expressions: they should generally remain within a factor $\sim 1.5-2$ from the exact values in the considered parameter range. Moreover, full nonlinear effects may modify the optimum value of $S^*$, and transverse propagation may hinder growth in the presence of corresponding inhomogeneities (neglected here). Finally, wave growth may also occur sensibly away from the equator, in which case terms $\partial\Omega_{ce}/\partial z$ may no longer be negligible [e.g., *Nunn and Omura*, 2012]. In the future, full-scale numerical simulations will therefore be needed to evaluate more precisely the nonlinear growth of very oblique lower band waves in various situations on the basis of full equations [*Nunn and Omura*, 2015].

**Acknowledgments**

The work at USTC was supported by the NSFC grants 41474125, 41331067, 11235009, and 41421063; Fundamental Research Funds for the Central Universities; Specialized Research Fund for State Key Laboratories; and Youth Innovation Promotion Association of Chinese Academy of Sciences (2016395). The work at UCLA was supported by NASA grants NNX15AF61G, NNX15AI96G, NNX13AI61G, and NNX14AI18G; AFOSR award FA9550-15-1-0158; and the NSF grants AGS 1405054, AGS 1564510, and PLR 1341359. We acknowledge NASA contract NAS5-02099 and V. Angelopoulos for use of data from the THEMIS Mission. Specifically, we thank J. W. Bonnell and F. S. Mozer for use of EFI data; A. Roux and O. LeContel for use of SCM data; and K. H. Glassmeier, U. Auster, and W. Baumjohann for the use of FGM data provided under the lead of the Technical University of Braunschweig and with financial support through the German Ministry for Economy and Technology and the German Center for Aviation and Space (DLR) under contract 50 OC 0302. The THEMIS data used in this study are obtained from http://themis.ssl.berkeley.edu/data/themis/.

## References

Agapitov, O. V., A. V. Artemyev, D. Mourenas, F. S. Mozer, and V. Krasnoselskikh (2015), Nonlinear local parallel acceleration of electrons through Landau trapping by oblique whistler mode waves in the outer radiation belt, *Geophys. Res. Lett.*, *42*, 10,140–10,149, doi:10.1002/2015GL066887.

Agapitov, O., V. Krasnoselskikh, Y. Zaliznyak, V. Angelopoulos, O. Le Contel, and G. Rolland (2011), Observations and modeling of forward and reflected chorus waves captured by THEMIS, *Ann. Geophys.*, *29*, 541–550, doi:10.5194/angeo-29-541-2011.

Agapitov, O., A. Artemyev, V. Krasnoselskikh, Y. V. Khotyaintsev, D. Mourenas, H. Breuillard, M. Balikhin, and G. Rolland (2013), Statistics of whistler mode waves in the outer radiation belt: Cluster STAFF-SA measurements, *J. Geophys. Res. Space Physics*, *118*, 3407–3420, doi:10.1002/jgra.50312.

An, X., B. Van Compernolle, J. Bortnik, R. M. Thorne, L. Chen, and W. Li (2016), Resonant excitation of whistler waves by a helical electron beam, *Geophys. Res. Lett.*, *43*, 2413–2421, doi:10.1002/2015GL067126.

Angelopoulos, V. (2008), The THEMIS mission, *Space Sci. Rev.*, *141*(1–4), 5–34, doi:10.1007/s11214-008-9336-1.

Artemyev, A. V., O. V. Agapitov, D. Mourenas, V. V. Krasnoselskikh, and F. S. Mozer (2015), Wave energy budget analysis in the Earth's radiation belts uncovers a missing energy, *Nat. Commun.*, *6*, 8143, doi:10.1038/ncomms8143.

Artemyev, A., V. Krasnoselskikh, O. Agapitov, D. Mourenas, and G. Rolland (2012), Non-diffusive resonant acceleration of electrons in the radiation belts, *Phys. Plasmas*, *19*, 122901, doi:10.1063/1.4769726.

Artemyev, A., O. Agapitov, D. Mourenas, V. Krasnoselskikh, V. Shastun, and F. Mozer (2016), Oblique whistler-mode waves in the Earth's inner magnetosphere: Energy distribution, origins, and role in radiation belt dynamics, *Space Sci. Rev.*, *200*, 261–355, doi:10.1007/s11214-016-0252-5.

Auster, H. U., et al. (2008), The THEMIS Fluxgate Magnetometer, *Space Sci. Rev.*, *141*(1–4), 235–264, doi:10.1007/s11214-008-9365-9.

Bonnell, J. W., F. S. Mozer, G. T. Delory, A. J. Hull, R. E. Ergun, C. M. Cully, V. Angelopoulos, and P. R. Harvey (2008), The Electric Field Instrument (EFI) for THEMIS, *Space Sci. Rev.*, *141*(1–4), 303–341, doi:10.1007/s11214-008-9469-2.

Bortnik, J., J. W. Cutler, C. Dunson, and T. E. Bleier (2007), An automatic wave detection algorithm applied to Pc1 pulsations, *J. Geophys. Res.*, *112*, A04204, doi:10.1029/2006JA011900.

Breuillard, H., O. Agapitov, A. Artemyev, V. Krasnoselskikh, O. Le Contel, C. M. Cully, V. Angelopoulos, Y. Zaliznyak, and G. Rolland (2014), On the origin of falling-tone chorus elements in Earth's inner magnetosphere, *Ann. Geophys.*, *32*, 1477–1485, doi:10.5194/angeo-32-1477-2014.

Chen, L., R. M. Thorne, W. Li, and J. Bortnik (2013), Modeling the wave normal distribution of chorus waves, *J. Geophys. Res. Space Physics*, *118*, 1074–1088, doi:10.1029/2012JA018343.

Demekhov, A. G. (2011), Generation of VLF emissions with the increasing and decreasing frequency in the magnetosperic cyclotron maser in the backward wave oscillator regime, *Radiophys. Quantum Electron.*, *53*, 609–622, doi:10.1007/s11141-011-9256-x.

Fu, X., et al. (2014), Whistler anisotropy instabilities as the source of banded chorus: Van Allen Probes observations and particle-in-cell simulations, *J. Geophys. Res. Space Physics*, *119*, 8288–8298, doi:10.1002/2014JA020364.

Gao, X., W. Li, R. M. Thorne, J. Bortnik, V. Angelopoulos, Q. Lu, X. Tao, and S. Wang (2014a), Statistical results describing the bandwidth and coherence coefficient of whistler mode waves using THEMIS waveform data, *J. Geophys. Res. Space Physics*, *119*, 8992–9003, doi:10.1002/2014JA020158.

Gao, X., W. Li, R. M. Thorne, J. Bortnik, V. Angelopoulos, Q. Lu, X. Tao, and S. Wang (2014b), New evidence for generation mechanisms of discrete and hiss-like whistler mode waves, *Geophys. Res. Lett.*, *41*, 4805–4811, doi:10.1002/2014GL060707.

Gao, X., Q. Lu, J. Bortnik, W. Li, L. Chen, and S. Wang (2016), Generation of multiband chorus by lower band cascade in the Earth's magnetosphere, *Geophys. Res. Lett.*, *43*, 2343–2350, doi:10.1002/2016GL068313.

Hall, D. S., C. P. Chaloner, D. A. Bryant, and D. R. Lepine (1991), Electrons in the boundary layers near the dayside magnetopause, *J. Geophys. Res.*, *96*, 7869–7891, doi:10.1029/90JA02137.

Hikishima, M., and Y. Omura (2012), Particle simulations of whistler-mode rising-tone emissions triggered by waves with different amplitudes, *J. Geophys. Res.*, *117*, A04226, doi:10.1029/2011JA017428.

Karpman, V. I., J. N. Istomin, and D. R. Shklyar (1974), Nonlinear frequency shift and self-modulation of the quasi-monochromatic whistlers in the inhomogeneous plasma (magnetosphere), *Planet. Space Sci.*, *22*, 859–871, doi:10.1016/0032-0633(74)90155-X.

Kennel, C. F., and F. Engelman (1966), Velocity space diffusion from weak plasma turbulence in a magnetic field, *Phys. Fluids*, *9*(12), 2377, doi:10.1063/1.1761629.

Kletzing, C. A. (1994), Electron acceleration by kinetic Alfven waves, *J. Geophys. Res.*, *99*, 11,095–11,103, doi:10.1029/94JA00345.

Kurita, S., H. Misawa, C. M. Cully, O. Le Contel, and V. Angelopoulos (2012), Source location of falling tone chorus, *Geophys. Res. Lett.*, *39*, L22102, doi:10.1029/2012GL053929.

Le Contel, O., et al. (2008), First results of the THEMIS search coil magnetometers, *Space Sci. Rev.*, *141*, 509–534, doi:10.1007/s11214-008-9371-y.

LeDocq, M. J., D. A. Gurnett, and G. B. Hospodarsky (1998), Chorus source locations from VLF Poynting flux measurements with the Polar spacecraft, *Geophys. Res. Lett.*, *25*(21), 4063–4066, doi:10.1029/1998GL900071.

Lee, L. C., J. R. Johnson, and Z. W. Ma (1994), Kinetic Alfven waves as a source of plasma transport at the dayside magnetopause, *J. Geophys. Res.*, *99*, 17,405–17,411, doi:10.1029/94JA01095.

Li, W., R. M. Thorne, V. Angelopoulos, J. Bortnik, C. M. Cully, B. Ni, O. LeContel, A. Roux, U. Auster, and W. Magnes (2009), Global distribution of whistler mode chorus waves observed on the THEMIS spacecraft, *Geophys. Res. Lett.*, *36*, L09104, doi:10.1029/2009GL037595.

Li, W., et al. (2010), THEMIS analysis of observed equatorial electron distributions responsible for the chorus excitation, *J. Geophys. Res.*, *115*, A00f11, doi:10.1029/2009JA014845.

Li, W., J. Bortnik, R. M. Thorne, and V. Angelopoulos (2011a), Global distribution of wave amplitudes and wave normal angles of chorus waves using THEMIS wave observations, *J. Geophys. Res.*, *116*, A12205, doi:10.1029/2011JA017035.
Li, W., R. M. Thorne, J. Bortnik, Y. Y. Shprits, Y. Nishimura, V. Angelopoulos, C. Chaston, O. Le Contel, and J. W. Bonnell (2011b), Typical properties of rising and falling tone chorus waves, *Geophys. Res. Lett.*, *38*, L14103, doi:10.1029/2011GL047925.
Li, W., R. M. Thorne, J. Bortnik, X. Tao, and V. Angelopoulos (2012), Characteristics of hiss-like and discrete whistler mode emissions, *Geophys. Res. Lett.*, *39*, L18106, doi:10.1029/2012GL053206.
Li, W., J. Bortnik, R. M. Thorne, C. M. Cully, L. Chen, V. Angelopoulos, Y. Nishimura, J. B. Tao, J. W. Bonnell, and O. Le Contel (2013), Characteristics of the Poynting flux and wave normal vectors of whistler-mode waves observed on THEMIS, *J. Geophys. Res. Space Physics*, *118*, 1461–1471, doi:10.1002/jgra.50176.
Li, W., et al. (2014), Evidence of stronger pitch angle scattering loss caused by oblique whistler-mode waves as compared with quasi-parallel waves, *Geophys. Res. Lett.*, *41*, 6063–6070, doi:10.1002/2014GL061260.
Li, W., O. Santolik, J. Bortnik, R. M. Thorne, C. A. Kletzing, W. S. Kurth, and G. B. Hospodarsky (2016), New chorus wave properties near the equator from Van Allen Probes wave observations, *Geophys. Res. Lett.*, *43*, 4725–4735, doi:10.1002/2016GL068780.
Malaspina, D. M., J. R. Wygant, R. E. Ergun, G. D. Reeves, R. M. Skoug, and B. A. Larsen (2015), Electric field structures and waves at plasma boundaries in the inner magnetosphere, *J. Geophys. Res. Space Physics*, *120*, 4246–4263, doi:10.1002/2015JA021137.
Mourenas, D., A. V. Artemyev, J.-F. Ripoll, O. V. Agapitov, and V. V. Krasnoselskikh (2012), Timescales for electron quasi-linear diffusion by parallel and oblique lower-band chorus waves, *J. Geophys. Res.*, *117*, A06234, doi:10.1029/2012JA017717.
Mourenas, D., A. Artemyev, O. Agapitov, and V. Krasnoselskikh (2014), Consequences of geomagnetic activity on energization and loss of radiation belt electrons by oblique chorus waves, *J. Geophys. Res. Space Physics*, *119*, 2775–2796, doi:10.1002/2013JA019674.
Mourenas, D., A. V. Artemyev, O. V. Agapitov, V. Krasnoselskikh, and F. S. Mozer (2015), Very oblique whistler generation by low-energy electron streams, *J. Geophys. Res. Space Physics*, *120*, 3665–3683, doi:10.1002/2015JA021135.
Mozer, F. S., O. V. Agapitov, A. Artemyev, J. F. Drake, V. Krasnoselskikh, S. Lejosne, and I. Vasko (2015), Time domain structures: What and where they are made, *Geophys. Res. Lett.*, *42*, 3627–3638, doi:10.1002/2015GL063946.
Ni, B. B., R. M. Thorne, Y. Y. Shprits, K. G. Orlova, and N. P. Meredith (2011), Chorus-driven resonant scattering of diffuse auroral electrons in nondipolar magnetic fields, *J. Geophys. Res.*, *116*, A06225, doi:10.1029/2011JA016453.
Nunn, D. (1971), A theory of VLF emissions, *Planet. Space Sci.*, *19*, 1141–1167, doi:10.1016/0032-0633(71)90110-3.
Nunn, D., and Y. Omura (2012), A computational and theoretical analysis of falling frequency VLF emissions, *J. Geophys. Res.*, *117*, A08228, doi:10.1029/2012JA017557.
Nunn, D., and Y. Omura (2015), A computational and theoretical investigation of nonlinear wave-particle interactions in oblique whistlers, *J. Geophys. Res. Space Physics*, *120*, 2890–2911, doi:10.1002/2014JA020898.
Omura, Y., and D. Nunn (2011), Triggering progress of whistler mode chorus emissions in the magnetosphere, *J. Geophys. Res.*, *116*, A05205, doi:10.1029/2010JA016280.
Omura, Y., Y. Katoh, and D. Summers (2008), Theory and simulation of the generation of whistler mode chorus, *J. Geophys. Res.*, *113*, A04223, doi:10.1029/2007JA012622.
Omura, Y., M. Hikishima, Y. Katoh, D. Summers, and S. Yagitani (2009), Nonlinear mechanisms of lower-band and upper-band VLF chorus emissions in the magnetosphere, *J. Geophys. Res.*, *114*, A07217, doi:10.1029/2009JA014206.
Omura, Y., D. Nunn, and D. Summers (2012), Generation processes of whistler mode chorus emissions: Current status of nonlinear wave growth theory, in *Dynamics of the Earth's Radiation Belts and Inner Magnetosphere*, *Geophys. Monogr. Ser.*, vol. 199, edited by D. Summers, et al., pp. 243-254, AGU, Washington, D. C., doi:10.1029/2012GM001347.
Parrot, M., O. Santolik, N. Cornilleau-Wehrlin, M. Maksimovic, and C. Harvey (2003), Magnetospherically reflected chorus waves revealed by ray tracing with CLUSTER data, *Ann. Geophys.*, *21*, 1111–1120, doi:10.5194/angeo-21-1111-2003.
Santolik, O., D. A. Gurnett, J. S. Pickett, M. Parrot, and N. Cornilleau-Wehirlin (2005), Central position of the source region of storm-time chorus, *Planet. Space Sci.*, *53*, 299–305, doi:10.1016/j.pss.2004.09.056.
Santolik, O., D. A. Gurnett, J. S. Pickett, J. Chum, and N. Cornilleau-Wehrlin (2009), Oblique propagation of whistler mode waves in the chorus source region, *J. Geophys. Res.*, *114*, A00f03, doi:10.1029/2009JA014586.
Shklyar, D., and H. Matsumoto (2009), Oblique whistler-mode waves in the inhomogeneous magnetospheric plasma: Resonant interactions with energetic charged particles, *Surv. Geophys.*, *30*, 55–104, doi:10.1007/s10712-009-9061-7.
Summers, D., C. Ma, N. P. Meredith, R. B. Horne, R. M. Thorne, D. Heynderickx, and R. R. Anderson (2002), Model of the energization of outer-zone electrons by whistler mode chorus during the October 9, 1990 geomagnetic storm, *Geophys. Res. Lett.*, *29*(24), 2174, doi:10.1029/2002GL016039.
Taubenschuss, U., Y. V. Khotyaintsev, O. Santolík, A. Vaivads, C. M. Cully, O. Le Contel, and V. Angelopoulos (2014), Wave normal angles of whistler mode chorus rising and falling tones, *J. Geophys. Res. Space Physics*, *119*, 9567–9578, doi:10.1002/2014JA020575.
Thorne, R. M., B. B. Ni, X. Tao, R. B. Horne, and N. P. Meredith (2010), Scattering by chorus waves as the dominant cause of diffuse auroral precipitation, *Nature*, *467*(7318), 943–946, doi:10.1038/Nature09467.
Thorne, R. M., et al. (2013), Rapid local acceleration of relativistic radiation-belt electrons by magnetospheric chorus, *Nature*, *504*(7480), 411, doi:10.1038/Nature12889.
Trakhtengerts, V. Y., A. G. Demekhov, E. E. Titova, B. V. Kozelov, O. Santolik, D. Gurnett, and M. Parrot (2004), Interpretation of Cluster data on chorus emissions using the backward wave oscillator model, *Phys. Plasmas*, *11*, 1345–1351, doi:10.1063/1.1667495.
Tsurutani, B. T., and E. J. Smith (1974), Postmidnight chorus – A substorm phenomenon, *J. Geophys. Res.*, *79*(1), 118–127, doi:10.1029/Ja079i001p00118.
Verkhoglyadova, O. P., B. T. Tsurutani, and G. S. Lakhina (2010), Properties of obliquely propagating chorus, *J. Geophys. Res.*, *115*, A00F19, doi:10.1029/2009JA014809.
Williams, D. J., D. G. Mitchell, T. E. Eastman, and L. A. Frank (1985), Energetic particle observations in the low-latitude boundary layer, *J. Geophys. Res.*, *90*, 5097–5116, doi:10.1029/JA090iA06p05097.
Zheng, H., S. Y. Fu, Q. G. Zong, Z. Y. Pu, Y. F. Wang, and G. K. Parks (2012), Observations of ionospheric electron beams in the plasma sheet, *Phys. Rev. Lett.*, *109*, 205001, doi:10.1103/PhysRevLett.109.205001.